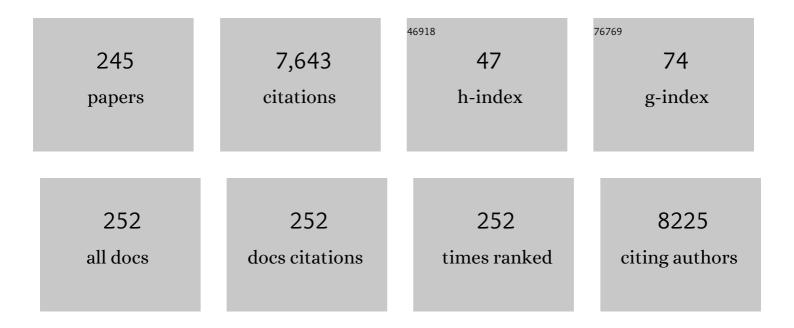
Gary J Cheng

List of Publications by Year in descending order

Source: https://exaly.com/author-pdf/2961971/publications.pdf Version: 2024-02-01



CADY | CHENC

#	Article	IF	CITATIONS
1	3D-printed hierarchical porous cellulose/alginate/carbon black hydrogel for high-efficiency solar steam generation. Chemical Engineering Journal, 2022, 430, 132765.	6.6	111
2	Highly sensitive and wide-range flexible pressure sensor based on carbon nanotubes-coated polydimethylsiloxane foam. Materials Letters, 2022, 308, 131151.	1.3	23
3	Bionic Optical Leaf for Photoreduction of CO ₂ from Noble Metal Atom Mediated Graphene Nanobubble Arrays. ACS Nano, 2022, 16, 1909-1918.	7.3	14
4	Self-packaged high-resolution liquid metal nano-patterns. Matter, 2022, 5, 1016-1030.	5.0	19
5	Understanding the role of monolayer graphene during long range shock strengthening of metal-graphene heterostructure. Materials Science & Engineering A: Structural Materials: Properties, Microstructure and Processing, 2022, 837, 142741.	2.6	4
6	An Ultrawideband GaAs MMIC Microstrip Directional Coupler With High Directivity and Very Flat Coupling. IEEE Transactions on Microwave Theory and Techniques, 2022, 70, 2271-2279.	2.9	5
7	High Power 10–18 GHz Monolithic Limiter Based on GaAs p-i-n Technology. IEEE Microwave and Wireless Components Letters, 2022, 32, 1107-1110.	2.0	3
8	Ultrahigh Sensitive Flexible Piezoresistive Sensor with Carbonized Metal–Organic Framework Fe ₃ O ₄ @MIL-100(Fe). ACS Applied Electronic Materials, 2022, 4, 1723-1731.	2.0	9
9	Origins of Ultrafast Pulse Laser-Induced Nano Straight Lines with Potential Applications in Detecting Subsurface Defects in Silicon Carbide Wafers. Nanomanufacturing and Metrology, 2022, 5, 167-178.	1.5	6
10	Nanoalloy libraries from laser-induced thermionic emission reduction. Science Advances, 2022, 8, eabm6541.	4.7	11
11	Carbon Black/Graphene Nanosheet Composites for Three-Dimensional Flexible Piezoresistive Sensors. ACS Applied Nano Materials, 2022, 5, 7142-7149.	2.4	22
12	A low-damage copper removal process by femtosecond laser for integrated circuits. Vacuum, 2022, 203, 111273.	1.6	7
13	Enhanced Energy Transfer from Nitrogenâ€Vacancy Centers to Threeâ€Dimensional Graphene Heterostructures by Laser Nanoshaping. Advanced Optical Materials, 2021, 9, 2001830.	3.6	12
14	Isolated atomic catalysts encapsulated in MOF for ultrafast water pollutant treatment. Nano Research, 2021, 14, 1287-1293.	5.8	11
15	Ultrafast transformation of Pbl ₂ in two-step fabrication of halide perovskite films for long-term performance and stability <i>via</i> nanosecond laser shock annealing. Journal of Materials Chemistry C, 2021, 9, 12819-12827.	2.7	8
16	Direct Ink Writing of Hierarchically Porous Cellulose/Alginate Monolithic Hydrogel as a Highly Effective Adsorbent for Environmental Applications. ACS Applied Polymer Materials, 2021, 3, 699-709.	2.0	58
17	Additive printing of recyclable anti-counterfeiting patterns with sol–gel cellulose nanocrystal inks. Nanoscale, 2021, 13, 11808-11816.	2.8	16
18	Ultrahigh Sensitivity Flexible Pressure Sensors Based on 3Dâ€Printed Hollow Microstructures for Electronic Skins. Advanced Materials Technologies, 2021, 6, 2000984.	3.0	44

#	Article	IF	CITATIONS
19	Controlled self-assembly of plasmon-based photonic nanocrystals for high performance photonic technologies. Nano Today, 2021, 37, 101072.	6.2	51
20	Understanding femtosecond laser internal scribing of diamond by atomic simulation: Phase transition, structure and property. Carbon, 2021, 175, 352-363.	5.4	13
21	Ultrastrong pure aluminum structure with gradient nanocrystals via selective pulsed laser melting: Computation framework and experiments. Journal of the Mechanics and Physics of Solids, 2021, 151, 104391.	2.3	6
22	A 3Dâ€Printed, Sensitive, Stable, and Flexible Piezoresistive Sensor for Health Monitoring. Advanced Engineering Materials, 2021, 23, 2100379.	1.6	19
23	Borophene via Micromechanical Exfoliation. Advanced Materials, 2021, 33, e2102039.	11.1	56
24	Ultrastrong medium entropy alloy with simultaneous strength-ductility improvement via heterogeneous nanocrystalline structures. Materials Science & Engineering A: Structural Materials: Properties, Microstructure and Processing, 2021, 823, 141631.	2.6	16
25	Ultrafast femtosecond pressure modulation of structure and exciton kinetics in 2D halide perovskites for enhanced light response and stability. Nature Communications, 2021, 12, 4879.	5.8	26
26	A 3D flexible piezoresistive sensor based on surface-filled graphene nanosheets conductive layer. Sensors and Actuators A: Physical, 2021, 332, 113144.	2.0	11
27	Silver nanowires interlocked graphene aerogel for ultra-high efficient clearage of oil pollution on water. Sustainable Materials and Technologies, 2021, 29, e00285.	1.7	2
28	A promising inorganic YFeO3 pigments with high near-infrared reflectance and infrared emission. Solar Energy, 2021, 226, 180-191.	2.9	17
29	Soap film inspired mechanical metamaterials approaching theoretical bound of stiffness across full density range. Materials Horizons, 2021, 8, 987-996.	6.4	18
30	Nanoscale-Precision Removal of Copper in Integrated Circuits Based on a Hybrid Process of Plasma Oxidation and Femtosecond Laser Ablation. Micromachines, 2021, 12, 1188.	1.4	4
31	3D MOF Nanoarchitecture Membrane via Ultrafast Laser Nanoforging. Small Methods, 2021, 5, e2100758.	4.6	8
32	Employing Hybrid Lennard-Jones and Axilrod-Teller Potentials to Parametrize Force Fields for the Simulation of Materials' Properties. Materials, 2021, 14, 6352.	1.3	4
33	Liquid metal nanolayer-linked MOF nanocomposites by laser shock evaporation. Matter, 2021, 4, 3977-3990.	5.0	17
34	Magnetically Aligned Ultrafine Cobalt Embedded 3D Porous Carbon Metamaterial by One‧tep Ultrafast Laser Direct Writing. Advanced Science, 2021, 8, e2102477.	5.6	9
35	Addressing the Reliability and Electron Transport Kinetics in Halide Perovskite Film via Pulsed Laser Engineering. Advanced Functional Materials, 2020, 30, 1906781.	7.8	24
36	Fabrication of 3D polymeric photonic arrays and related applications. Materials Today Chemistry, 2020, 15, 100208.	1.7	10

#	Article	IF	CITATIONS
37	An Acoustic Metaâ€Skin Insulator. Advanced Materials, 2020, 32, e2002251.	11.1	26
38	Quantum Dot Enabled Perovskite Thin Film with Enhanced Crystallization, Stability, and Carrier Diffusion via Pulsed Laser Nanoengineering. Advanced Materials Interfaces, 2020, 7, 2001021.	1.9	6
39	Parallel Nanoimprint Forming of One-Dimensional Chiral Semiconductor for Strain-Engineered Optical Properties. Nano-Micro Letters, 2020, 12, 160.	14.4	8
40	Stable mid-infrared polarization imaging based on quasi-2D tellurium at room temperature. Nature Communications, 2020, 11, 2308.	5.8	259
41	A Single-Atomic Noble Metal Enclosed Defective MOF via Cryogenic UV Photoreduction for CO Oxidation with Ultrahigh Efficiency and Stability. ACS Applied Materials & Interfaces, 2020, 12, 26068-26075.	4.0	34
42	A review on microstructures and properties of high entropy alloys manufactured by selective laser melting. International Journal of Extreme Manufacturing, 2020, 2, 032003.	6.3	69
43	Strainâ€Engineered Anisotropic Optical and Electrical Properties in 2D Chiralâ€Chain Tellurium. Advanced Materials, 2020, 32, e2002342.	11.1	40
44	Graphene-Metal-Metastructure Monolith via Laser Shock-Induced Thermochemical Stitching of MOF Crystals. Matter, 2020, 2, 1535-1549.	5.0	49
45	Controllable near-infrared reflectivity and infrared emissivity with substitutional iron-doped orthorhombic YMnO3 coatings. Solar Energy, 2020, 206, 778-786.	2.9	18
46	Highly Sensitive Flexible Piezoresistive Sensor with 3D Conductive Network. ACS Applied Materials & Interfaces, 2020, 12, 35291-35299.	4.0	81
47	Molecular-Scale Nanodiamond with High-Density Color Centers Fabricated from Graphite by Laser Shocking. Cell Reports Physical Science, 2020, 1, 100054.	2.8	4
48	Ultrahigh electrocatalytic activity with trace amounts of platinum loadings on free-standing mesoporous titanium nitride nanotube arrays for hydrogen evolution reactions. Nanoscale, 2020, 12, 15393-15401.	2.8	31
49	Ultrafast Laser Manufacture of Stable, Efficient Ultrafine Noble Metal Catalysts Mediated with MOF Derived High Density Defective Metal Oxides. Small, 2020, 16, e2000749.	5.2	31
50	Overview of Laser Applications in Manufacturing and Materials Processing in Recent Years. Journal of Manufacturing Science and Engineering, Transactions of the ASME, 2020, 142, .	1.3	29
51	Laser-Shock-Induced Nanoscale Kink-Bands in WSe2 2D Crystals. ACS Nano, 2019, 13, 10587-10595.	7.3	11
52	Roll to roll manufacturing of fast charging, mechanically robust 0D/2D nanolayered Si-graphene anode with well-interfaced and defect engineered structures. Energy Storage Materials, 2019, 22, 450-460.	9.5	31
53	Additive Printed All-Cellulose Membranes with Hierarchical Structure for Highly Efficient Separation of Oil/Water Nanoemulsions. ACS Applied Materials & Interfaces, 2019, 11, 44375-44382.	4.0	43
54	Photoplastic Transformation Based on Dynamic Covalent Chemistry. ACS Applied Materials & Amp; Interfaces, 2019, 11, 23623-23631.	4.0	18

#	Article	IF	CITATIONS
55	Asymmetric 3D Elastic–Plastic Strainâ€Modulated Electron Energy Structure in Monolayer Graphene by Laser Shocking. Advanced Materials, 2019, 31, e1900597.	11.1	32
56	Scalable Nanoshaping of Hierarchical Metallic Patterns with Multiplex Laser Shock Imprinting Using Soft Optical Disks. Small, 2019, 15, e1900481.	5.2	18
57	Artificial control of in-plane anisotropic photoelectricity in monolayer MoS2. Applied Materials Today, 2019, 15, 203-211.	2.3	45
58	Nanoscale Laser Metallurgy and Patterning in Air Using MOFs. Journal of the American Chemical Society, 2019, 141, 5481-5489.	6.6	61
59	Pulsed Laser Modulated Shock Transition from Liquid Metal Nanoparticles to Mechanically and Thermally Robust Solid–Liquid Patterns. Advanced Materials, 2019, 31, e1807811.	11.1	55
60	Double-negative-index ceramic aerogels for thermal superinsulation. Science, 2019, 363, 723-727.	6.0	429
61	Laser Shock Tuning Dynamic Interlayer Coupling in Graphene–Boron Nitride Moiré Superlattices. Nano Letters, 2019, 19, 283-291.	4.5	31
62	Straining effects in MoS ₂ monolayer on nanostructured substrates: temperature-dependent photoluminescence and exciton dynamics. Nanoscale, 2018, 10, 5717-5724.	2.8	54
63	Composite bending-dominated hollow nanolattices: A stiff, cyclable mechanical metamaterial. Materials Today, 2018, 21, 467-474.	8.3	26
64	Ultrafast Laserâ€6hockâ€Induced Confined Metaphase Transformation for Direct Writing of Black Phosphorus Thin Films. Advanced Materials, 2018, 30, 1704405.	11.1	17
65	Alpha Lead Oxide (αâ€₽bO): A New 2D Material with Visible Light Sensitivity. Small, 2018, 14, e1703346.	5.2	58
66	Largeâ€Area Direct Laserâ€Shock Imprinting of a 3D Biomimic Hierarchical Metal Surface for Triboelectric Nanogenerators. Advanced Materials, 2018, 30, 1705840.	11.1	93
67	Shock engineering the additive manufactured graphene-metal nanocomposite with high density nanotwins and dislocations for ultra-stable mechanical properties. Acta Materialia, 2018, 150, 360-372.	3.8	77
68	Dry Etching with Nanoparticles: Formation of High Aspectâ€Ratio Pores and Channels Using Magnetic Gold Nanoclusters. Advanced Materials, 2018, 30, 1703091.	11.1	11
69	Enhancement of osteoblast activity on nanostructured NiTi/hydroxyapatite coatings on additive manufactured NiTi metal implants by nanosecond pulsed laser sintering. International Journal of Nanomedicine, 2018, Volume 13, 8217-8230.	3.3	16
70	Optoelectronic performance enhancement in pulsed laser deposited gallium-doped zinc oxide (GZO) films after UV laser crystallization. Applied Physics A: Materials Science and Processing, 2018, 124, 1.	1.1	5
71	Laser Sintering of Liquid Metal Nanoparticles for Scalable Manufacturing of Soft and Flexible Electronics. ACS Applied Materials & Interfaces, 2018, 10, 28232-28241.	4.0	189
72	Molten salt synthesis of YMnO3 powder with high near-infrared reflectivity. Materials Letters, 2018, 229, 171-173.	1.3	10

#	Article	IF	CITATIONS
73	Ultrastrong nanocrystalline stainless steel and its Hall-Petch relationship in the nanoscale. Scripta Materialia, 2018, 155, 26-31.	2.6	72
74	Tunable random lasing behavior in plasmonic nanostructures. Nano Convergence, 2017, 4, 1.	6.3	54
75	Flyweight, Superelastic, Electrically Conductive, and Flameâ€Retardant 3D Multiâ€Nanolayer Graphene/Ceramic Metamaterial. Advanced Materials, 2017, 29, 1605506.	11.1	89
76	In vitro osteoblast gene expression and differentiation atop of titanium blocks laser coated with multilayer biphasic calcium phosphate/titanium nanocomposites. Biomedical Physics and Engineering Express, 2017, 3, 025022.	0.6	0
77	Defects Mediated Corrosion in Graphene Coating Layer. ACS Applied Materials & Interfaces, 2017, 9, 11902-11908.	4.0	48
78	Lasing behavior of surface functionalized carbon quantum dot/RhB composites. Nanoscale, 2017, 9, 5049-5054.	2.8	21
79	Laser additive manufacturing bulk graphene–copper nanocomposites. Nanotechnology, 2017, 28, 445705.	1.3	30
80	Graphene/PbS-Quantum Dots/Graphene Sandwich Structures Enabled by Laser Shock Imprinting for High Performance Photodetectors. ACS Applied Materials & Interfaces, 2017, 9, 44715-44723.	4.0	49
81	A reusable laser wrapped graphene-Ag array based SERS sensor for trace detection of genomic DNA methylation. Biosensors and Bioelectronics, 2017, 92, 755-762.	5.3	81
82	3D nanostructured inkjet printed graphene via UV-pulsed laser irradiation enables paper-based electronics and electrochemical devices. Nanoscale, 2016, 8, 15870-15879.	2.8	108
83	Three-dimensional-linked carbon fiber-carbon nanotube hybrid structure for enhancing thermal conductivity of silicon carbonitride matrix composites. Carbon, 2016, 108, 38-46.	5.4	61
84	Observation of Optical and Electrical In-Plane Anisotropy in High-Mobility Few-Layer ZrTe ₅ . Nano Letters, 2016, 16, 7364-7369.	4.5	80
85	Additive roll printing activated cold welding of 2D crystals and 1D nanowires layers for flexible transparent conductor and planer energy storage. Extreme Mechanics Letters, 2016, 9, 531-545.	2.0	12
86	Mesoporous nitrogen-doped carbon hollow spheres as high-performance anodes for lithium-ion batteries. Journal of Power Sources, 2016, 324, 233-238.	4.0	108
87	Numerical simulation of temperature field distribution for laser sintering graphene reinforced nickel matrix nanocomposites. Journal of Alloys and Compounds, 2016, 688, 438-448.	2.8	5
88	Superplastic Formation of Metal Nanostructure Arrays with Ultrafine Gaps. Advanced Materials, 2016, 28, 9152-9162.	11.1	24
89	Controlled and Stabilized Light–Matter Interaction in Graphene: Plasmonic Film with Large cale 10â€nm Lithography. Advanced Optical Materials, 2016, 4, 1811-1823.	3.6	28
90	Parallel Nanoshaping of Brittle Semiconductor Nanowires for Strained Electronics. Nano Letters, 2016, 16, 7536-7544.	4.5	21

#	Article	IF	CITATIONS
	xmlns:mml="http://www.w3.org/1998/Math/MathML" altimg="si1.gif" display="inline" overflow="scroll"> <mml:msub><mml:mrow><mml:mstyle< td=""><td></td><td></td></mml:mstyle<></mml:mrow></mml:msub>		
91	mathvariant="normal"> <mml:mi>Bi</mml:mi> <mml:mrow><mml:mi>x</mml:mi>mathvariant="normal"><mml:mi>Sb</mml:mi></mml:mrow> <mml:mrow><mml:mn>2</mml:mn><td>2.0 ml:mrow</td><td>> {/mml:msu</td></mml:mrow>	2.0 ml:mrow	> {/mml:msu
	Extreme Mechanics Letters, 2016, 9, 386-396.		a
92	Fluorescence Lifetime Imaging of Nanoflares for mRNA Detection in Living Cells. Analytical Chemistry, 2016, 88, 1979-1983.	3.2	34
93	Spectral plasmonic effect in the nano-cavity of dye-doped nanosphere-based photonic crystals. Nanotechnology, 2016, 27, 165703.	1.3	12
	Nanotechnology, 2010, 27, 105705.		
94	Laser sintered graphene nickel nanocomposites. Journal of Materials Processing Technology, 2016, 231,	3.1	59
	143-150.		
95	Ultrafast direct fabrication of flexible substrate-supported designer plasmonic nanoarrays.	2.8	40
20	Nanoscale, 2016, 8, 172-182.	2.0	ч 0
0.6	[INVITED] A review: Warm laser shock peening and related laser processing technique. Optics and Laser		
96	Technology, 2016, 78, 15-24.	2.2	99
	Welding of Semiconductor Nanowires by Coupling Laser-Induced Peening and Localized Heating.		
97	Scientific Reports, 2015, 5, 16052.	1.6	8
	Super-strengthening and stabilizing with carbon nanotube harnessed high density nanotwins in		
98	metals by shock loading. Scientific Reports, 2015, 5, 15405.	1.6	38
99	Large Scale Laser Crystallization of Solution-based Alumina-doped Zinc Oxide (AZO) Nanoinks for Highly Transparent Conductive Electrode. Scientific Reports, 2015, 5, 15517.	1.6	17
100	Highly transparent conductive electrode with ultra-low HAZE by grain boundary modification of aqueous solution fabricated alumina-doped zinc oxide nanocrystals. APL Materials, 2015, 3, 062803.	2.2	24
101	Enhanced Multiphoton Emission from CdTe/ZnS Quantum Dots Decorated on Single-Layer Graphene. Journal of Physical Chemistry C, 2015, 119, 6331-6336.	1.5	24
102	Pulse laser deposition fabricated InP/Al-ZnO heterojunction solar cells with efficiency enhanced by an i-ZnO interlayer. Applied Physics A: Materials Science and Processing, 2015, 121, 1219-1226.	1.1	6
	an Perio Intenayer. Applied Physics A. Materials Science and Processing, 2013, 121, 1219-1220.		
103	3D stereolithography printing of graphene oxide reinforced complex architectures. Nanotechnology,	1.3	177
	2015, 26, 434003.		
104	Laser Shock-Induced Conformal Transferring of Functional Devices on 3-D Stretchable Substrates.	1.7	6
104	Journal of Microelectromechanical Systems, 2015, 24, 414-421.	1.7	0
	Laser direct writing of crystalline Fe2O3 atomic sheets on steel surface in aqueous medium. Applied		
105	Surface Science, 2015, 351, 148-154.	3.1	17
	Crystalline Nanojoining Silver Nanowire Percolated Networks on Flexible Substrate. ACS Nano, 2015,		
106	9, 10018-10031.	7.3	84
	Maccocols elucidation of logar assisted observices days etting of Company transferred electron days		
107	Mesoscale elucidation of laser-assisted chemical deposition of Sn nanostructured electrodes. Journal of Applied Physics, 2015, 117, 214301.	1.1	2
108	Preparation and Effect of Lighting on Structures and Properties of GSH Capped ZnSe QDs. Journal of Fluorescence, 2015, 25, 1663-1669.	1.3	6

#	Article	IF	CITATIONS
109	Single-Layer Graphene as a Barrier Layer for Intense UV Laser-Induced Damages for Silver Nanowire Network. ACS Nano, 2015, 9, 11121-11133.	7.3	59
110	Graphene laminated gold bipyramids as sensitive detection platforms for antibiotic molecules. Chemical Communications, 2015, 51, 15494-15497.	2.2	55
111	Crystalline photoactive copper indium diselenide thin films by pulsed laser crystallization of nanoparticle-inks at ambient conditions. RSC Advances, 2015, 5, 57550-57558.	1.7	4
112	Water flattens graphene wrinkles: laser shock wrapping of graphene onto substrate-supported crystalline plasmonic nanoparticle arrays. Nanoscale, 2015, 7, 19885-19893.	2.8	41
113	Enhanced Multi-Photon Emission from Single NV Center Coupled to Graphene by Laser-Shaping. , 2015, ,		0
114	Laser Crystallization of Transparent AZO Films on Sapphire With High Electron Mobility for Photo-Application. , 2014, , .		0
115	Cryogenic ultrahigh strain rate deformation induced hybrid nanotwinned microstructure for high strength and high ductility. Journal of Applied Physics, 2014, 115, .	1.1	34
116	Development of ZnO-InP heterojunction solar cells for thin film photovoltaics. , 2014, , .		2
117	Charge carrier transport and collection enhancement of copper indium diselenide photoactive nanoparticle-ink by laser crystallization. Applied Physics Letters, 2014, 105, .	1.5	11
118	Large-scale nanoshaping of ultrasmooth 3D crystalline metallic structures. Science, 2014, 346, 1352-1356.	6.0	153
119	Ultraviolet laser crystallized ZnO:Al films on sapphire with high Hall mobility for simultaneous enhancement of conductivity and transparency. Applied Physics Letters, 2014, 104, .	1.5	36
120	Laser sintering of separated and uniformly distributed multiwall carbon nanotubes integrated iron nanocomposites. Journal of Applied Physics, 2014, 115, .	1.1	22
121	Transparent and antibacterial Cu2Y2O5 thin films by chemical solution deposition. Thin Solid Films, 2014, 570, 547-551.	0.8	6
122	Ultrafast and scalable laser liquid synthesis of tin oxide nanotubes and its application in lithium ion batteries. Nanoscale, 2014, 6, 5853-5858.	2.8	36
123	Enhancing photo-induced ultrafast charge transfer across heterojunctions of CdS and laser-sintered TiO ₂ nanocrystals. Physical Chemistry Chemical Physics, 2014, 16, 10669-10678.	1.3	10
124	Magnetic field assisted growth of highly dense α-Fe ₂ O ₃ single crystal nanosheets and their application in water treatment. RSC Advances, 2014, 4, 18621-18626.	1.7	16
125	Three-Dimensional Printing of Complex Structures: Man Made or toward Nature?. ACS Nano, 2014, 8, 9710-9715.	7.3	72
126	Precise selective scribing of thin-film solar cells by a picosecond laser. Applied Physics A: Materials Science and Processing, 2014, 116, 671-681.	1.1	13

#	Article	IF	CITATIONS
127	Single-layer graphene oxide reinforced metal matrix composites by laser sintering: Microstructure and mechanical property enhancement. Acta Materialia, 2014, 80, 183-193.	3.8	158
128	Ultrahigh dense and gradient nano-precipitates generated by warm laser shock peening for combination of high strength and ductility. Materials Science & Engineering A: Structural Materials: Properties, Microstructure and Processing, 2014, 609, 195-203.	2.6	97
129	Magnetic Field Assisted Growth of High Dense Hematite Nanosheets and Their Application in Water Treatment. , 2014, , .		0
130	Control of Ablation Depth and Surface Structure in P3 Scribing of Thin-Film Solar Cells by a Picosecond Laser. Journal of Micro and Nano-Manufacturing, 2014, 2, .	0.8	5
131	Control of Ablation Depth and Surface Structure in P3 Scribing of Thin-Film Solar Cells by a Picosecond Laser. , 2014, , .		0
132	Direct Laser Writing of Nanodiamond Films from Graphite under Ambient Conditions. Scientific Reports, 2014, 4, 6612.	1.6	27
133	Pulsed laser induced confined vapor deposition for thin layer of dense nanoparticle arrays on various substrates. Applied Surface Science, 2013, 283, 924-929.	3.1	8
134	Controlled precipitation by thermal engineered laser shock peening and its effect on dislocation pinning: Multiscale dislocation dynamics simulation and experiments. Acta Materialia, 2013, 61, 1957-1967.	3.8	41
135	Plasmonic tuning of silver nanowires by laser shock induced lateral compression. Nanoscale, 2013, 5, 6311.	2.8	13
136	Direct Integration of Functional Structures on 3-D Microscale Surfaces by Laser Dynamic Forming. Journal of Microelectromechanical Systems, 2013, 22, 1428-1437.	1.7	3
137	Laser assisted electro-deposition of earth abundant Cu2ZnSnS4 photovoltaic thin film. Manufacturing Letters, 2013, 1, 54-58.	1.1	10
138	Mechanism of fatigue performance enhancement in a laser sintered superhard nanoparticles reinforced nanocomposite followed by laser shock peening. Journal of Applied Physics, 2013, 113, .	1.1	32
139	Electropulsing induced crystal orientation change and its effects on electric conductivity of nanofilms of Zn–Al alloys. Applied Physics A: Materials Science and Processing, 2013, 111, 1241-1245.	1.1	6
140	The Investigation of Plasma Produced by Intense Nanosecond Laser Ablation in Vacuum Under External Magnetic Field Using a Two-Stage Model. Journal of Manufacturing Science and Engineering, Transactions of the ASME, 2013, 135, .	1.3	3
141	Magnetic Field Effects on Laser Drilling. Journal of Manufacturing Science and Engineering, Transactions of the ASME, 2013, 135, .	1.3	32
142	Direct pulsed laser crystallization of nanocrystals for absorbent layers in photovoltaics: Multiphysics simulation and experiment. Journal of Applied Physics, 2013, 113, 193506.	1.1	9
143	Laser and Photonic Systems Integration: Emerging Innovations and Framework for Research and Education. Human Factors and Ergonomics in Manufacturing, 2013, 23, 483-516.	1.4	7
144	Mechanism of Fatigue Performance Enhancement in a Superhard Nanoparticles Integrated Nanocomposites by a Hybrid Manufacturing Technique. , 2013, , .		2

#	Article	IF	CITATIONS
145	Enhanced Laser Shock by an Active Liquid Confinement—Hydrogen Peroxide. Journal of Manufacturing Science and Engineering, Transactions of the ASME, 2012, 134, .	1.3	9
146	Finite Element Analysis of the Variation in Residual Stress Distribution in Laser Shock Peening of Steels. Journal of Manufacturing Science and Engineering, Transactions of the ASME, 2012, 134, .	1.3	19
147	Effects of rapid thermal processing and pulse-laser sintering on CdTe nanofilms for photovoltaic applications. , 2012, , .		6
148	Direction-tunable nanotwins in copper nanowires by laser-assisted electrochemical deposition. Nanotechnology, 2012, 23, 125602.	1.3	8
149	Direct writing of Au nanoneedles array on glass by confined laser spinning. Applied Physics Letters, 2012, 101, 091911.	1.5	1
150	Deformation induced martensite in NiTi and its shape memory effects generated by low temperature laser shock peening. Journal of Applied Physics, 2012, 112, .	1.1	38
151	Free standing GaN nano membrane by laser lift-off method. Materials Research Society Symposia Proceedings, 2012, 1432, 53.	0.1	4
152	Deposition of Al-Doped Zinc Oxide by Direct Pulsed Laser Recrystallization at Room Temperature on Various Substrates for Solar Cell Applications. , 2012, , .		0
153	Laser Shock Induced Nano-Patterning of Graphene. , 2012, , .		Ο
154	Nanotwins in Copper Nanowires Controlled by Laser Assisted Electrochemical Deposition. , 2012, , .		0
155	Enhanced Laser Shock by an Active Liquid Confinement. , 2012, , .		Ο
156	Effect of Warm Laser Shock Peening on the Tensile Strength and Ductility of Aluminum Alloys. , 2012, ,		0
157	Room temperature deposition of alumina-doped zinc oxide on flexible substrates by direct pulsed laser recrystallization. Applied Physics Letters, 2012, 100, .	1.5	24
158	The mechanisms of thermal engineered laser shock peening for enhanced fatigue performance. Acta Materialia, 2012, 60, 4997-5009.	3.8	74
159	Laser assisted embedding of nanoparticles into metallic materials. Applied Surface Science, 2012, 258, 2289-2296.	3.1	17
160	Large scale, highly dense nanoholes on metal surfaces by underwater laser assisted hydrogen etching near nanocrystalline boundary. Applied Surface Science, 2012, 258, 4254-4259.	3.1	8
161	Scalable patterning on shape memory alloy by laser shock assisted direct imprinting. Applied Surface Science, 2012, 258, 10042-10046.	3.1	33
162	An eXtended Finite Element Method (XFEM) study on the effect of reinforcing particles on the crack propagation behavior in a metal–matrix composite. International Journal of Fatigue, 2012, 44, 151-156.	2.8	54

#	Article	lF	CITATIONS
163	Nanoscale Strainability of Graphene by Laser Shock-Induced Three-Dimensional Shaping. Nano Letters, 2012, 12, 4577-4583.	4.5	47
164	Nanoparticles Embedding Into Metallic Materials by Laser Direct Irradiation. , 2012, , .		0
165	Deformation-induced martensite and nanotwins by cryogenic laser shock peening of AISI 304 stainless steel and the effects on mechanical properties. Philosophical Magazine, 2012, 92, 1369-1389.	0.7	55
166	Laser Shock-Based Platform for Controllable Forming of Nanowires. Nano Letters, 2012, 12, 3224-3230.	4.5	21
167	Surface form memory in NiTi shape memory alloys by laser shock indentation. Journal of Materials Science, 2012, 47, 2088-2094.	1.7	16
168	Laser Engineered Multilayer Coating of Biphasic Calcium Phosphate/Titanium Nanocomposite on Metal Substrates. ACS Applied Materials & Interfaces, 2011, 3, 339-350.	4.0	36
169	Scalable nano-patterning of graphenes using laser shock. Nanotechnology, 2011, 22, 475303.	1.3	11
170	Stability, Antimicrobial Activity, and Cytotoxicity of Poly(amidoamine) Dendrimers on Titanium Substrates. ACS Applied Materials & Interfaces, 2011, 3, 2885-2894.	4.0	52
171	Continuous Mode Laser Coating of Hydroxyapatite/Titanium Nanoparticles on Metallic Implants: Multiphysics Simulation and Experimental Verification. Journal of Manufacturing Science and Engineering, Transactions of the ASME, 2011, 133, .	1.3	5
172	Pulsed Laser Coating of Hydroxyapatite/Titanium Nanoparticles on Ti-6Al-4V Substrates: Multiphysics Simulation and Experiments. IEEE Transactions on Nanobioscience, 2011, 10, 177-186.	2.2	7
173	3D microscale laser dynamic forming: Multiscale modeling and experimental validation. Journal of Applied Physics, 2011, 109, .	1.1	11
174	Nanoscale Size Dependence on Metallic Nanoparticles: Case Study of Titanium Nanoparticles on Pulsed Laser Sintering of Hydroxyapatite/Titanium Nanoparticles. , 2011, , .		0
175	Bimodal nanocrystallization of NiTi shape memory alloy by laser shock peening and post-deformation annealing. Acta Materialia, 2011, 59, 7219-7227.	3.8	120
176	Fatigue performance improvement in AISI 4140 steel by dynamic strain aging and dynamic precipitation during warm laser shock peening. Acta Materialia, 2011, 59, 1014-1025.	3.8	230
177	Dense and uniform Au nanospheres on glass through confined nanosecond pulsed laser irradiation. Applied Physics Letters, 2011, 99, 091901.	1.5	3
178	Dislocation pinning effects induced by nano-precipitates during warm laser shock peening: Dislocation dynamic simulation and experiments. Journal of Applied Physics, 2011, 110, .	1.1	35
179	Highly conductive and transparent alumina-doped ZnO films processed by direct pulsed laser recrystallization at room temperature. Applied Physics Letters, 2011, 99, .	1.5	34
180	Microstructure and mechanical properties of copper subjected to cryogenic laser shock peening. Journal of Applied Physics, 2011, 110, .	1.1	46

#	Article	IF	CITATIONS
181	The Effect of External Magnetic Field on the Plasma Induced by Laser Ablation in Vacuum. , 2011, , .		3
182	Controlled Nanocrystallization of NiTi Shape Memory Alloy by Laser Shock Peening. , 2011, , .		0
183	Laser Shock Based Controlled Forming of Silver Nanowires. , 2011, , .		0
184	Direct pulsed laser crystallization of copper indium diselenide nanocrystal thin films for photovoltaics. , 2011, , .		0
185	Stagnation Pressure in Liquid Needle-Free Injection: Modeling and Experimental Validation. Drug Delivery Letters, 2011, 1, 97-104.	0.2	6
186	Stagnation Pressure in Liquid Needle-Free Injection: Modeling and Experimental Validation. Drug Delivery Letters, 2011, 1, 97-104.	0.2	1
187	Forming Limit and Fracture Mode of Microscale Laser Dynamic Forming. Journal of Manufacturing Science and Engineering, Transactions of the ASME, 2010, 132, .	1.3	38
188	Laser Coating of HAp/Ti Nanoparticles on Metal Implants: Interfacial Bonding Strength, Chemical Analysis and Biocompatibility. , 2010, , .		0
189	Effect of Multiple Pulses on the Deformation Behavior of Ultrathin Metal Foils in 3D Micro-Scale Laser Dynamic Forming. , 2010, , .		0
190	Fatigue Performance Improvement by Dynamic Strain Aging and Dynamic Precipitation in Warm Laser Shock Peening of AISI 4140 Steel. , 2010, , .		5
191	Nucleation of Highly Dense Nanoscale Precipitates Based on an Innovative Process: Warm Laser Shock Peening. , 2010, , .		1
192	Experiment, thermal simulation, and characterizations on transmission laser coating of hydroxyapatite on metal implant. Journal of Biomedical Materials Research - Part A, 2010, 92A, 70-79.	2.1	15
193	Warm Laser Shock Peening Driven Nanostructures and Their Effects on Fatigue Performance in Aluminum Alloy 6160. Advanced Engineering Materials, 2010, 12, 291-297.	1.6	50
194	Environmental assessment of laser assisted manufacturing: case studies on laser shock peening and laser assisted turning. Journal of Cleaner Production, 2010, 18, 1311-1319.	4.6	46
195	Functionalization of micro- and nano-apertures with chromate-selective solvent polymeric membrane. Analytica Chimica Acta, 2010, 659, 243-250.	2.6	3
196	Nucleation of highly dense nanoscale precipitates based on warm laser shock peening. Journal of Applied Physics, 2010, 108, .	1.1	47
197	A Model on Liquid Penetration Into Soft Material With Application to Needle-Free Jet Injection. Journal of Biomechanical Engineering, 2010, 132, 101005.	0.6	19
198	Laser Shock Peening of Nanoparticles Integrated Alloys: Numerical Simulation and Experiments. Journal of Manufacturing Science and Engineering, Transactions of the ASME, 2010, 132, .	1.3	6

#	Article	IF	CITATIONS
199	A Dislocation Dynamics Based Constitutive Model and Experimental Validations by 3D Microscale Laser Dynamic Forming of Metallic Thin Films. , 2010, , .		0
200	Effects of Temperature on Laser Shock Induced Plastic Deformation: The Case of Copper. Journal of Manufacturing Science and Engineering, Transactions of the ASME, 2010, 132, .	1.3	28
201	Nanoscale size dependence on pulsed laser sintering of hydroxyapatite/titanium particles on metal implants. Journal of Applied Physics, 2010, 108, 113112.	1.1	13
202	Multiple-pulse laser dynamic forming of metallic thin films for microscale three dimensional shapes. Journal of Applied Physics, 2010, 108, .	1.1	22
203	Laser-Induced High-Strain-Rate Superplastic 3-D Microforming of Metallic Thin Films. Journal of Microelectromechanical Systems, 2010, 19, 273-281.	1.7	47
204	Intelligent Energy Field Manufacturing. , 2010, , .		9
205	Forming limit and fracture mode of microscale laser dynamic forming. , 2010, , .		0
206	Laser-Induced Plastic Deformation and Its Applications. , 2010, , 299-318.		0
207	Numerical Simulation on Nanoparticles Integrated Laser Shock Peening of Aluminum Alloy. , 2009, , .		0
208	Microstructure and texture developments in multiple pulses excimer laser crystallization of GaAs thin films. Journal of Applied Physics, 2009, 105, .	1.1	9
209	Laser dynamic forming of functional materials laminated composites on patterned three-dimensional surfaces with applications on flexible microelectromechanical systems. Applied Physics Letters, 2009, 95, 091108.	1.5	27
210	Modeling and Analysis of Liquid Penetration into Soft Material with Application to Needle-Free Jet Injection. , 2009, , .		1
211	Deformation Modes in Stainless Steel During Laser Shock Peening. Journal of Manufacturing Science and Engineering, Transactions of the ASME, 2009, 131, .	1.3	6
212	Deformation Behaviors and Critical Parameters in Microscale Laser Dynamic Forming. Journal of Manufacturing Science and Engineering, Transactions of the ASME, 2009, 131, .	1.3	43
213	Multilayer Laser Sintering of HAp/Ti Nanoparticles Onto Metallic Implants. , 2009, , .		1
214	Multiphysics simulation on electromagnetic peening of predrilled holes. International Journal of Mechanical Sciences, 2009, 51, 825-836.	3.6	11
215	Bilayer lipid membrane (BLM) based ion selective electrodes at the meso-, micro-, and nano-scales. Biosensors and Bioelectronics, 2009, 24, 1843-1849.	5.3	37
216	Laser Induced High-Strain-Rate Superplastic 3D Micro-Forming of Metallic Thin Film. , 2009, , .		0

#	Article	IF	CITATIONS
217	Plastic Deformation in Silicon Crystal Induced by Heat-Assisted Laser Shock Peening. Journal of Manufacturing Science and Engineering, Transactions of the ASME, 2008, 130, .	1.3	30
218	Experiment, Thermal Simulation and Characterizations on Transmission Laser Coating of Hydroxyapatite on Metal Implant. , 2008, , .		0
219	Numerical Investigation of Temperature Field During Sintering of Bioceramic Nanoparticles by Pulse Lasers. , 2008, , .		1
220	Nanoparticle Heat Transfer and Its Application to Laser Hyperthermia. , 2007, , 1093.		3
221	Effect of film thickness and laser energy density on the microstructure of a-GaAs films after excimer laser crystallization. Journal of Applied Physics, 2007, 102, 013519.	1.1	6
222	Microstructure and mechanical property characterizations of metal foil after microscale laser dynamic forming. Journal of Applied Physics, 2007, 101, 063108.	1.1	89
223	Microstructure-properties relationship in two Al-Mg-Si alloys through a combination of extrusion and aging. Jom, 2007, 59, 58-61.	0.9	15
224	Characterizations on Microscale Laser Dynamic Forming of Metal Foil. , 2006, , 29.		1
225	Numerical Simulation on Short Pulsed Laser Heating of Semiconductor Thin Films: The Case of GaAs. , 2006, , 241.		0
226	Multiscale dislocation dynamics analyses of laser shock peening in silicon single crystals. International Journal of Plasticity, 2006, 22, 2171-2194.	4.1	36
227	Feasibility study of a smart motion generator utilizing electromagnetic microactuator arrays. Smart Materials and Structures, 2006, 15, 859-868.	1.8	2
228	Effect of Film Thickness and Laser Energy Density on the Structural Characteristics of Laser-Annealed Polycrystalline Gallium Arsenide Films. , 2006, , .		0
229	A Hybrid Rapid Microfluidic Mixer Utilizing Electrokinetic Relay and Asymmetric Flow Geometries for Lab-on-a-Chip Applications. , 2005, , 233.		0
230	Bioceramic coating of hydroxyapatite on titanium substrate with Nd-YAG laser. Materials Science and Engineering C, 2005, 25, 541-547.	3.8	97
231	Dislocation behavior in silicon crystal induced by laser shock peening: A multiscale simulation approach. Scripta Materialia, 2005, 53, 1013-1018.	2.6	33
232	Experimental study and computer simulation of fracture toughness of sheet metal after laser forming. International Journal of Advanced Manufacturing Technology, 2005, 26, 1222-1230.	1.5	14
233	Design and fabrication of a hybrid nanofluidic channel. Journal of Micro/ Nanolithography, MEMS, and MOEMS, 2005, 4, 013009.	1.0	10
234	Low-temperature crystallized pyrochlore bismuth zinc niobate thin films by excimer laser annealing. Applied Physics Letters, 2005, 87, 232905.	1.5	36

#	Article	IF	CITATIONS
235	Combined research and curriculum development of nontraditional manufacturing. European Journal of Engineering Education, 2005, 30, 363-376.	1.5	13
236	Fatigue Life Prediction After Laser Forming. Journal of Manufacturing Science and Engineering, Transactions of the ASME, 2005, 127, 157-164.	1.3	11
237	Process synthesis of laser forming by genetic algorithm. International Journal of Machine Tools and Manufacture, 2004, 44, 1619-1628.	6.2	33
238	Process Design of Laser Forming for Three-Dimensional Thin Plates. Journal of Manufacturing Science and Engineering, Transactions of the ASME, 2004, 126, 217-225.	1.3	44
239	Analytical and finite element model pull-in study of rigid and deformable electrostatic microactuators. Journal of Micromechanics and Microengineering, 2004, 14, 57-68.	1.5	104
240	Experimental study and computer simulation on fracture toughness of sheet metal after laser forming. , 2003, , .		0
241	Fatigue life prediction after laser forming. , 2003, , .		0
242	Microstructure Integrated Modeling of Multiscan Laser Forming. Journal of Manufacturing Science and Engineering, Transactions of the ASME, 2002, 124, 379-388.	1.3	55
243	Cooling Effects in Multiscan Laser Forming. Journal of Manufacturing Processes, 2001, 3, 60-72.	2.8	77
244	Process synthesis of laser forming by genetic algorithm. , 2001, , .		2
245	Precipitation strengthening of stress-aged Al–xCu alloys. Acta Materialia, 2000, 48, 2239-2246.	3.8	120